Hindawi
Mathematical Problems in Engineering
Volume 2018, Article ID 1539849, 10 pages
https://doi.org/10.1155/2018/1539849

Research Article

Generation and Meshing Analysis of a New Type of Double Helical Gear Transmission

Dong Liang,[1,2] **Tianhong Luo**,[1] **and Rulong Tan**[3]

[1] *School of Mechanotronics & Vehicle Engineering, Chongqing Jiaotong University, No. 66 Xuefu Street, Nan'an District, Chongqing 400074, China*
[2] *The Key Laboratory of Expressway Construction Machinery of Shanxi Province, Chang'an University, Middle-Section of Nan'er Huan Road Xi'an, Shanxi 710064, China*
[3] *The State Key Laboratory of Mechanical Transmission, Chongqing University, No. 174 Shazheng Street, Shapingba District, Chongqing 400030, China*

Correspondence should be addressed to Dong Liang; cqjtuliangdong_me@163.com

Received 6 March 2018; Revised 3 June 2018; Accepted 11 June 2018; Published 13 September 2018

Academic Editor: Francesco Franco

A study on the double helical gear transmission with curve element constructed tooth pairs is carried out in this paper. Generation and mathematical model of tooth profiles are proposed based on the geometric relationship. Tooth profiles equations are derived considering the developed equidistance-enveloping approach. Design of tooth profiles with point contact is conducted and numerical example is illustrated. And the solid models of double helical gear pair with curve element constructed tooth pairs are established. Computerized design and meshing simulation are also put forward. Furthermore, stress analysis of the gear pair is conducted and gear prototypes are manufactured using CNC machining technology. Further tooth contact analysis, dynamic and experimental studies on transmission properties of gear prototypes will be carried out.

1. Introduction

New types of gear drive are currently research focus for high transmission performance requirements. Various theories, design, and analysis approaches were provided by researchers. Utilizing the face-milling cutter, Fuentes et al. [1] put forward general geometric descriptions of circular arc gears with curvilinear teeth. Generation process of gear pair was given. Meshing simulation and tooth contact analysis were also carried out. Considering the intermediary helicoid as basic generation, using the established circular arc profile in axle plane, Dudás [2] presented the mathematical model and motion simulation of a worm gear drive. Based on the theory of gear kinematics, Zimmer et al. [3] derived a mathematical framework to calculate geometric relationships of arbitrary gear types and the general algorithms were illustrated. Kahraman [4] developed a family of torsional dynamic models of compound gear sets to predict the free vibration characteristics under different kinematic configurations resulting in different speed ratios. The compound gear sets considered consist of two planes of single- or double-planet gear sets connected by a straight long planet. Kahraman [5] also provided a model to predict load-dependent (mechanical) power losses of spur gear pairs based on an elastohydrodynamic lubrication (EHL) model. Simon [6] put forward a new type of cylindrical worm gear drive. The worm is ground by a grinding wheel of a double arc profile, and the obtained worm profile is concave. The teeth of the gear are processed by a hob whose generator surface corresponds to the worm surface. Simon [7] also developed the design and manufacturing methods of the hob for processing a worm gear with circular axial profile. Bahk et al. [8] investigated the impact of tooth profile modification on spur planetary gear vibration. The analytical model was proposed to capture the excitation from tooth profile modifications at the sun-planet and ring-planet meshes. Song et al. [9] designed the conjugated straight-line internal gear pairs for fluid power gear machines. The conjugated straight-line internal gear pair includes a pinion with straight-line profile and an internal gear with profile conjugated to the pinion profile.

Huang et al. [10] proposed an internal mesh planetary gear with small tooth number difference (PGSTD), and dynamic characteristics analysis was carried out. Lin [11] provided a new non-circular bevel gear based on the combination of cam mechanism and non-circular bevel gear.

For double helical gear drive, it has currently attracted more attentions in the field of low speed and heavy load machinery. Sondkar et al. [12] established the dynamic model of double helical planetary gear pair. A linear, time-invariant form was developed and further studies on dynamic characteristics were carried out. Zhang et al. [13] investigated the computerized design and simulation of meshing of modified double circular arc helical gears by tooth end relief with helix. The proposed theory was illustrated with numerical examples which confirm the advantages of the gear drives of the modified geometry. According to the characteristic of tooth profile modification, Wang et al. [14] presented the method of three-segment modification for pinion profile. The optimization results of tooth profile and axial modification without consideration of axes error can reduce the loaded transmission error. Kawasaki et al. [15, 16] proposed a manufacturing method of double helical gears using a multiaxis control and multitasking machine tool. The pitch errors, tooth thickness, runout, profile, lead, and surface roughness of manufactured double helical gears were also measured. Otherwise, the relationship between the tool wear and life time of the end mill was made clear. And the manufacturing method was applied to the gears for a double helical gear pump.

To obtain the better transmission performance and to meet the higher strength requirements, a new double helical gear transmission with curve element constructed tooth pairs is studied in this paper. Generation principle and mathematical model of this gear drive are provided. Numerical example is illustrated in terms of the established tooth profiles form. Computerized design and meshing simulation are also put forward. Furthermore, stress analysis of the gear pair is conducted and gear prototypes are manufactured using CNC machining technology.

2. Generation and Mathematical Model of Tooth Profiles

2.1. Contact Principle. Contact curves of tooth profiles are defined with three parts: spatial helix curve Γ_1, spatial helix curve Γ_2, and circular arc curve Γ_3. The spatial helix curve Γ_1 and the spatial helix curve Γ_2 are symmetric curves relative to the middle section of tooth width. The circular arc curve Γ_3 is the smooth transition curve connecting the curves Γ_1 and Γ_2.

The spatial helix curves Γ_1 and Γ_2 are expressed as follows:

$$\Gamma_i : \begin{cases} x_i = R_r \cos\theta_{ri} \\ y_i = R_r \sin\theta_{ri} \\ z_i = p_r \theta_{ri} \end{cases} \qquad (i = 1, 2) \tag{1}$$

where R_r is cylinder helix radius, θ_{ri} (i=1, 2) is spatial helix curve parameter, and p_r is helix parameter.

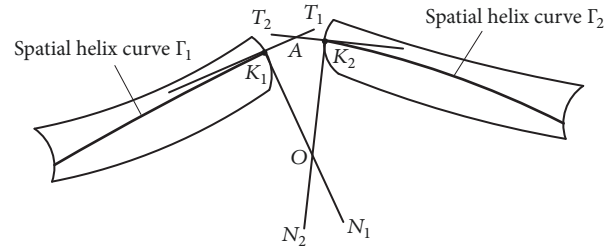

Figure 1: Geometric relationship.

Transition circular arc curve Γ_3 is derived by mathematic approach and its location plane needs to be first determined. As shown in Figure 1, T_1 and T_2 are the tangent at points K_1 and K_2 on the spatial helix curves Γ_1 and Γ_2, respectively. The two lines are given to the A point. The normal lines at points K_1 and K_2 are expressed using N_1, N_2. The two lines are given to the O point.

According to (1), its derivative can be calculated as

$$\begin{aligned} x'_i &= -R_r \sin\theta_{ri} \\ y'_i &= R_r \cos\theta_{ri} \\ z'_i &= p_r \\ &\qquad (i = 1, 2) \end{aligned} \tag{2}$$

and, at point K_1, we have the coordinate results (x_{k1}, y_{k1}, z_{k1}) and $(x'_{k1}, y'_{k1}, z'_{k1})$. So the equation of tangent T_1 is shown as

$$\frac{x - x_{k1}}{x'_{k1}} = \frac{y - y_{k1}}{y'_{k1}} = \frac{z - z_{k1}}{z'_{k1}} \tag{3}$$

Similarly, the equation of tangent T_2 is expressed as

$$\frac{x - x_{k2}}{x'_{k2}} = \frac{y - y_{k2}}{y'_{k2}} = \frac{z - z_{k2}}{z'_{k2}} \tag{4}$$

With simultaneous equations (3) and (4), the value of point A can be obtained. Obviously, normal lines N_1, N_2 are determined based on the above tangent expressions.

Normal line N_1:

$$(x - x_{k1})\, x'_{k1} + (y - y_{k1})\, y'_{k1} + (z - z_{k1})\, z'_{k1} = 0 \tag{5}$$

Normal line N_2:

$$(x - x_{k2})\, x'_{k2} + (y - y_{k2})\, y'_{k2} + (z - z_{k2})\, z'_{k2} = 0 \tag{6}$$

In simultaneous equations (5) and (6), the family of point O can be calculated and the point meeting the actual requirements will be further determined by the following conditions.

A plane can be generated at three points in space. As shown in Figure 2, suppose that the intersection point O is the circle center and the circular arc curve passing points K_1 and K_2 is drawn and it should satisfy the constant tangents T_1 and T_2.

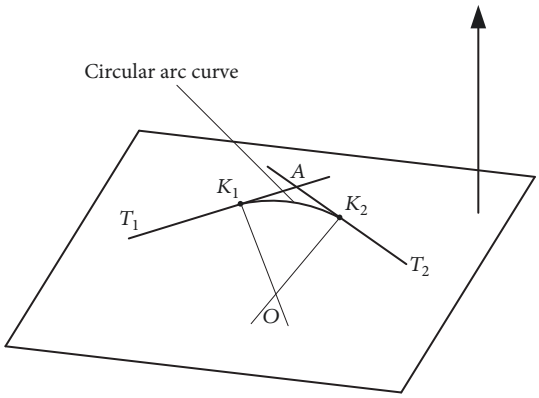

Figure 2: Determination of circular arc curve.

The normal vector at the location plane of circular arc curve can be represented using the developed tangent conditions as

$$\begin{aligned} \boldsymbol{t_1} &= (x_A - x_{k1})\,\boldsymbol{i} + (y_A - y_{k1})\,\boldsymbol{j} + (z_A - z_{k1})\,\boldsymbol{k} \\ \boldsymbol{t_2} &= (x_A - x_{k2})\,\boldsymbol{i} + (y_A - y_{k2})\,\boldsymbol{j} + (z_A - z_{k2})\,\boldsymbol{k} \\ \boldsymbol{n} &= \boldsymbol{t_1} \times \boldsymbol{t_2} \end{aligned} \tag{7}$$

Using the normal condition, it also can be written as

$$\begin{aligned} \boldsymbol{n_1} &= (x_O - x_{k1})\,\boldsymbol{i} + (y_O - y_{k1})\,\boldsymbol{j} + (z_O - z_{k1})\,\boldsymbol{k} \\ \boldsymbol{n_2} &= (x_O - x_{k2})\,\boldsymbol{i} + (y_O - y_{k2})\,\boldsymbol{j} + (z_O - z_{k2})\,\boldsymbol{k} \\ \boldsymbol{n}' &= \boldsymbol{n_1} \times \boldsymbol{n_2} \end{aligned} \tag{8}$$

Considering that the results of (7) and (8) are simplified to unit vectors, it should meet the expression $\boldsymbol{n} \bullet \boldsymbol{n}' = 1$. Then, the point O (x_O, y_O, z_O) can be obtained in terms of aforementioned conclusion.

The location plane of circular arc curve is provided as

$$\boldsymbol{n}\left[(x - x_{k1})\,\boldsymbol{i} + (y - y_{k1})\,\boldsymbol{j} + (z - z_{k1})\,\boldsymbol{k}\right] = 0 \tag{9}$$

We can find that the angle between plane $y_1O_1z_1$ and the location plane yOz of circular arc curve is φ, as displayed in Figure 3. It can be calculated through the normal vectors of the plane $y_1O_1z_1$ and the plane yOz, and it has

$$\cos\varphi = \frac{\boldsymbol{n} \bullet \boldsymbol{N}}{|\boldsymbol{n}| \bullet |\boldsymbol{N}|} \tag{10}$$

The circular arc curve in coordinate system $S(O\text{-}x,y,z)$ is expressed as

$$\begin{aligned} x &= 0 \\ y &= -r\cos\delta \\ z &= r\sin\delta \end{aligned} \tag{11}$$

where r is the radius of circular arc and δ is in the range $-\arctan(z_{k2}/y_{k2}) \le \delta \le \arctan(z_{k2}/y_{k2})$. Further, based on the coordinate transformation, the equation of circular arc curve Γ_3 is written as

$$\begin{aligned} x_3 &= r\cos\delta\sin\varphi + x_O \\ y_3 &= -r\cos\delta\cos\varphi + y_O \\ z_3 &= r\sin\delta \end{aligned} \tag{12}$$

According to the developed equidistance-enveloping approach [17, 18], the tubular meshing tooth profiles are generated and general equations of tooth profiles for spatial helix curve Γ_1, spatial helix curve Γ_2, and circular arc curve Γ_3 are

$$\Sigma_i: \begin{cases} x_{\Sigma i} = R_r\cos\theta_{ri} + h\left(n^0_{nx1} + \cos\varphi_1\cos\alpha_1\right) \\ y_{\Sigma i} = R_r\sin\theta_{ri} + h\left(n^0_{ny1} + \cos\varphi_1\sin\alpha_1\right) \\ z_{\Sigma i} = p_r\theta_{ri} + h\left(n^0_{nz1} + \sin\varphi_1\right) \\ \left(-R_r\sin\theta_{ri} + h{n^0_{nx1}}'\right)\cos\alpha_1 + \left(R_r\cos\theta_{ri} + h{n^0_{ny1}}'\right)\sin\alpha_1 \\ +\left(p_r + h{n^0_{nz1}}'\right)\tan\varphi_1 = 0 \end{cases} \tag{13}$$

$(i = 1, 2)$

and

$$\Sigma_3: \begin{cases} x_{\Sigma 3} = r\cos\delta\sin\varphi + x_O + h\left(n^0_{nx1} + \cos\varphi_1\cos\alpha_1\right) \\ y_{\Sigma 3} = -r\cos\delta\cos\varphi + y_O + h\left(n^0_{ny1} + \cos\varphi_1\sin\alpha_1\right) \\ z_{\Sigma 3} = r\sin\delta + h\left(n^0_{nz1} + \sin\varphi_1\right) \\ \left(-r\sin\delta\sin\varphi + h{n^0_{nx1}}'\right)\cos\alpha_1 + \left(r\sin\delta\cos\varphi + h{n^0_{ny1}}'\right)\sin\alpha_1 \\ +r\cos\delta\tan\varphi_1 = 0 \end{cases} \tag{14}$$

where h is the given equidistance with respect to the contact curves, $n^0_{nx1}, n^0_{ny1}, n^0_{nz1}$ are the unit components of normal vector. And sphere expression in (13) and (14) is written using $(h\cos\varphi_1\cos\alpha_1, h\cos\varphi_1\sin\alpha_1, h\sin\varphi_1)$.

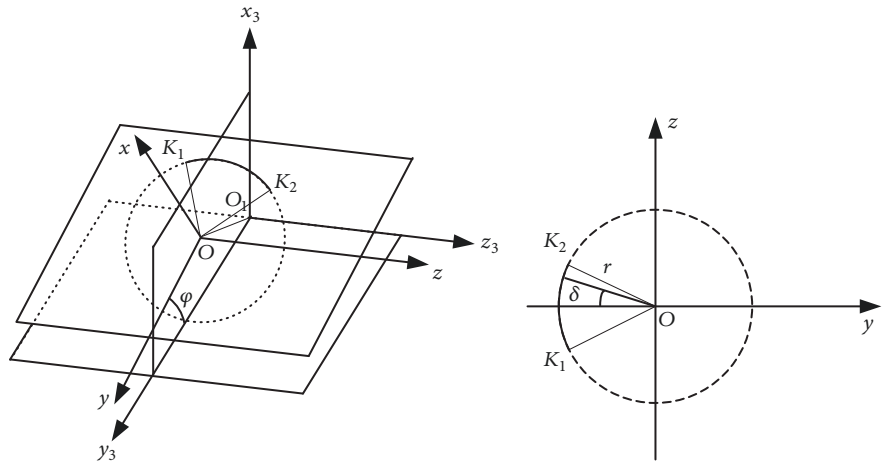

(a) Position relationship between plane $y_1O_1z_1$ and plane yOz

(b) Circular arc curve on plane yOz

Figure 3: Equation derivation of circular arc curve.

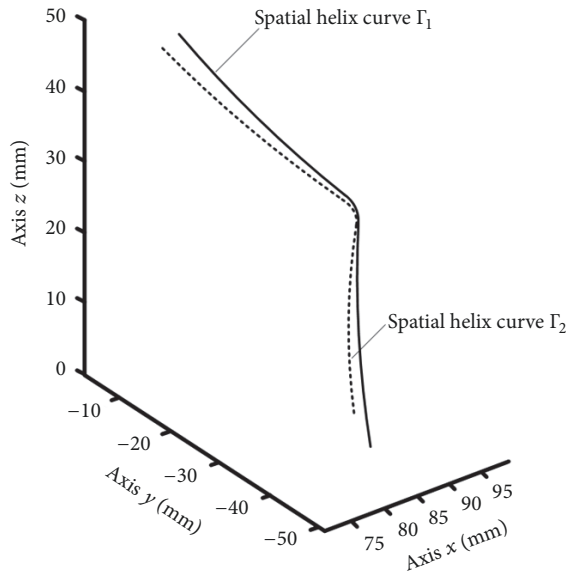

Figure 4: Engagement of spatial helix conjugate curves.

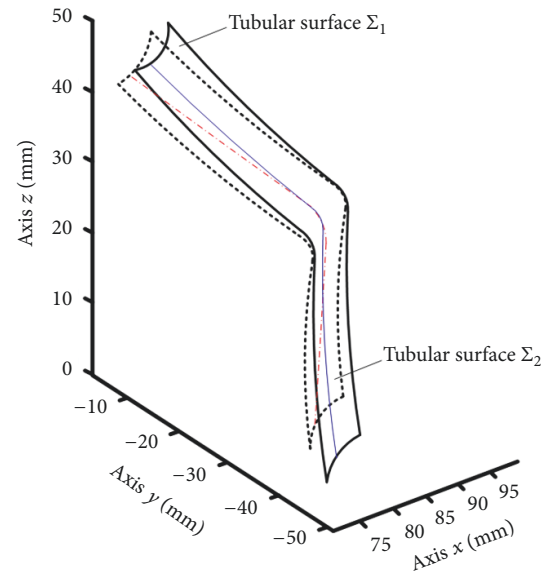

Figure 5: Engagement of tubular surfaces generated by MATLAB.

Parameters such as $R_r = 12mm$, $Z_1 = 6$, $Z_2 = 30$, $a = 72mm$, $i_{21} = 0.2$, $p_r = 28.6479$ and $0 \le \theta_r \le 1.0472rad$ are given, where R_r is cylinder helix radius, Z_1 and Z_2 are the number of teeth for pinion and gear, a is central distance, i_{21} is gear ratio, p_r is helix parameter, and θ_r is curve parameter angle. We obtain the engagement drawing results shown in Figures 4 and 5 using MATLAB software.

2.2. Design of Tooth Profiles. In this paper, normal section of convex-to-concave tooth profiles is provided. The main engagement region is set to the parabolic curves and basic parametric design of tooth profiles is given in Table 1. Meanwhile, the scheme of tooth profiles is depicted in Figure 6.

The left or right tooth profiles of double helical gear drive contact in point which is also the common tangent point. The double helical gear drive with curve element constructed tooth pairs is generated and it can be expressed in Figure 7.

For general conjugate surface theory, tooth profiles mainly are generated based on the given surface 1 and the established meshing relationship. And the only generated surface 2 is fixed. However, for conjugate curve theory, tooth profiles inheriting meshing characteristics of the conjugate curves are generated based on the given curve 1. The generated tooth profiles can be diversity if choosing the different curve form and contact position. Comparisons of two kinds of generation theory are shown in Figure 8.

Compared with the existing gears, the new type of gear pair may have the following characteristics: (1) few teeth number and large module may be obtained without tooth undercutting. (2) The special meshing of generated convex

Table 1: Parametric design of normal section of tooth profiles.

Parametric design	Symbols	Pinion tooth profile	Gear tooth profile
Normal modulus	m_n		
Pressure angle	α	18° ~36°	18° ~36°
Tooth height	h_1, h_2	$(1.3\sim1.5)m_n$	$(1.34\sim1.54)m_n$
Radius of tooth profile curve	ρ_a, ρ_f	$(1.3\sim1.5)m_n$	$(1.34\sim1.54)m_n$
Circle centre movement distance	e_a, e_f	0	$0.01m_n$
Circle centre offset distance	l_a, l_f	$0.59m_n$	$0.55m_n$
Distance linking contact point and pitch curve	h_k	$0.63m_n$	$0.63m_n$
Tooth thick at contact point	S_a, S_f	$1.54m_n$	$1.54m_n$
Tooth space at contact point	ω_{ak}, ω_{fk}	$1.6m_n$	$1.54m_n$
Tooth crack	j	0	$0.05m_n$
Addendum chamfer angle of gear tooth	γ_e		45°
Addendum chamfer height of gear tooth	h_e		$0.16m_n$

Table 2: Mathematical parameters for generating the gear pair.

Parameters	Symbols	Values
Radius of pitch circle of pinion (mm)	R_{r1}	18.5
Radius of pitch circle of gear (mm)	R_{r2}	92.5
Normal module (mm)	m_n	6
Pinion tooth number	Z_1	6
Gear tooth number	Z_2	30
Pressure angle (°)	α_α	25
Gear ratio	i_{21}	5
Tooth profile radius of pinion (mm)	ρ_a	9
Tooth profile radius of gear (mm)	ρ_f	9.9
Helix parameter	P	28.6478
Pinion equidistant distance (mm)	D_{h1}	9
Gear equidistant distance (mm)	D_{h2}	9.9
Tooth width (mm)	B	40
Curve parameter range (rad)	θ	0~1.048

and concave tooth profiles makes relative radius of curvature of the contact point longer and increases the contact strength. The load capacity will be improved. (3) The tooth profiles mesh in point contact along the conjugate curves, and the approximate pure rolling contact between mating tooth surfaces may occur.

2.3. Numerical Example. Numerical example is illustrated according to the developed tooth profiles equations. Through the generation idea shown in Figure 9, we establish the solid models of double helical gear pair in terms of mathematical parameters in Table 2. And the results are displayed in Figure 10.

Computerized engagement motion of tooth profiles is simulated and the results show that gear pair rotates with a fixed transmission ratio and continuous motion. For the axial direction, tooth profiles mesh in point contact and there is no engagement interference during the mated gear pair.

3. Meshing Analysis of Tooth Profiles

3.1. Force Analysis. Force conditions of tooth profiles in the normal direction are analyzed in Figure 11 and they are summarized as follows.

(1) Circumferential force F_{ti} is

$$F_{ti} = \frac{2T_i}{d_i} \quad (i = pinion\ 1, \text{gear}\ 2) \tag{15}$$

(2) Axial force F_{ai} is

$$F_{ai} = F_{ti} \tan\beta \quad (i = pinion\ 1, \text{gear}\ 2) \tag{16}$$

(3) Radial force F_{ri} is

$$F_{ri} = \frac{F_{ti} \tan\alpha_n}{\cos\beta} \quad (i = pinion\ 1, \text{gear}\ 2) \tag{17}$$

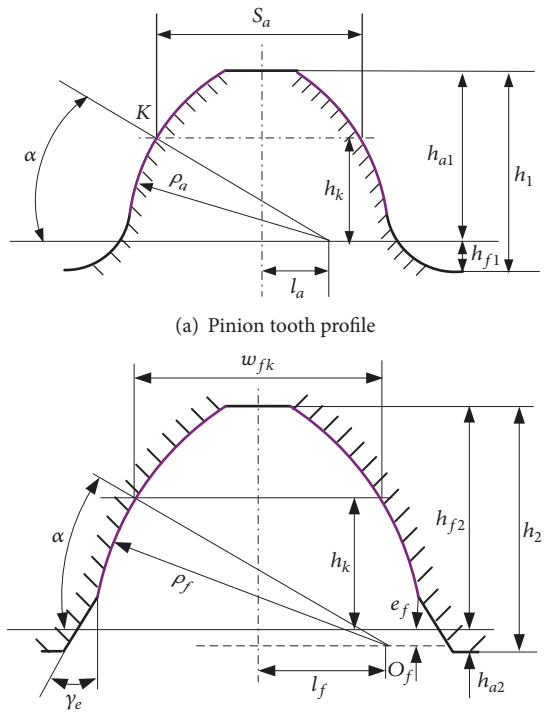

(a) Pinion tooth profile

(b) Gear tooth profile

FIGURE 6: Normal section of tooth profiles.

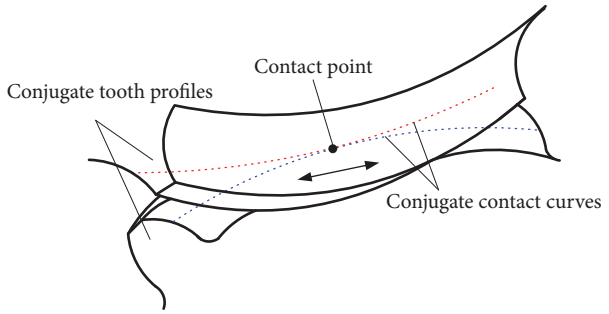

FIGURE 7: Double helical gears with curve element constructed tooth pairs.

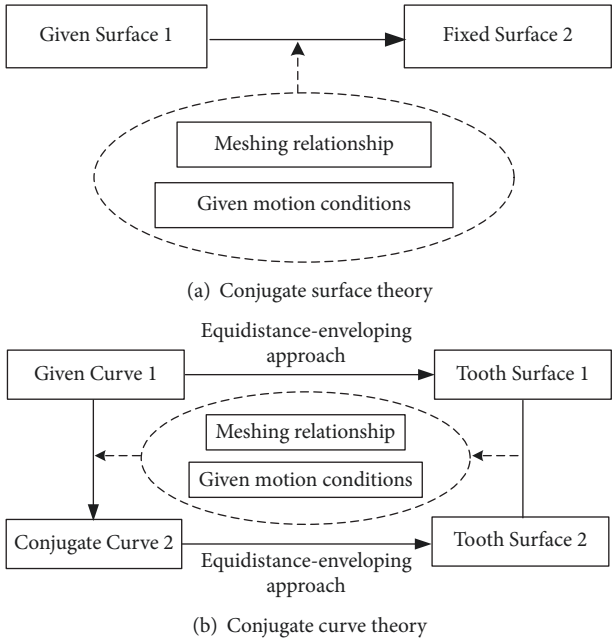

FIGURE 8: Comparisons of two kinds of generation theory.

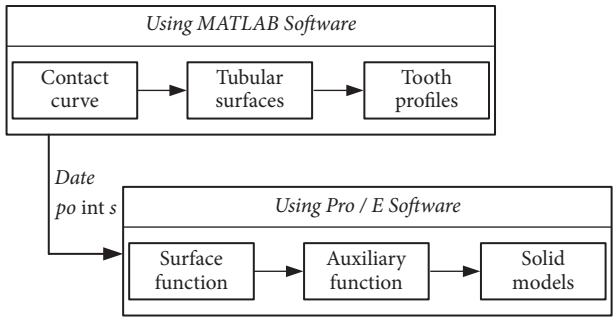

FIGURE 9: Generation idea of solid models.

Then, the normal force in name is expressed as follows:

$$F_{ni} = \frac{F_{ti}}{\cos\alpha_t \cos\beta_b} \quad (i = pinion\ 1, \text{gear}\ 2) \tag{18}$$

where T is the moment of force. β is helix angle and β_b is the helix angle in pitch circle. α_t is pressure angle in end and α_n is pressure angle in normal.

3.2. Stress Evaluation Using FEA. Stress analysis of teeth of gear pair is carried out and ANSYS software is utilized to analyze the process. To get ideal results of contact position and to guarantee of calculation precision, we take one side of tooth profiles as the object.

Considering the actual engagement conditions, gear pair is plotted with hexahedron unit Solid185 using Hypermesh software. The network should be densely drawn due to stress convergence and contact position change. The unit size of contact area is set as 0.2mm. Supposing that tooth profiles of the pinion and gear are the contact surfaces and target surface, respectively, we adopt the Contact 173 and Targe 170 forms as the contact units for them. In addition, engagement action is assumed as standard and the contact stiffness factor in normal section is 1. Pin connection and multipoint constraint are, respectively, applied to the engagement pair. The gear inner surface unit and its rotational center are fixed. Hertz model is applied to analysis process of contact stress. Using the extended Lagrange algorithm and Mpc 184 constraint unit to the analysis process, finite element model of conjugate pair is established in Figure 12. In this process, 20CrMnTi material whose properties are v=0.25, E=207GPa is selected.

Torque applied to the gear is 1250Nm and angular velocity applied to the pinion is 0.85rad/s. Finite element analysis results of tooth profiles are obtained in Figure 13. The gear pair shows point contact characteristic on the surface of contact

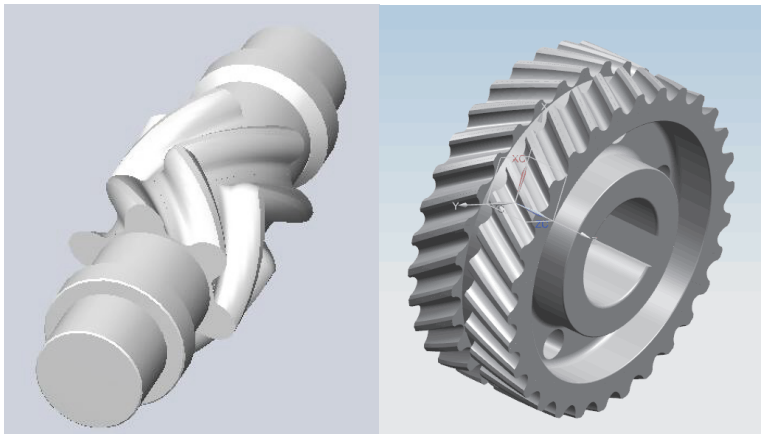

Figure 10: Solid models of double helical gear pair.

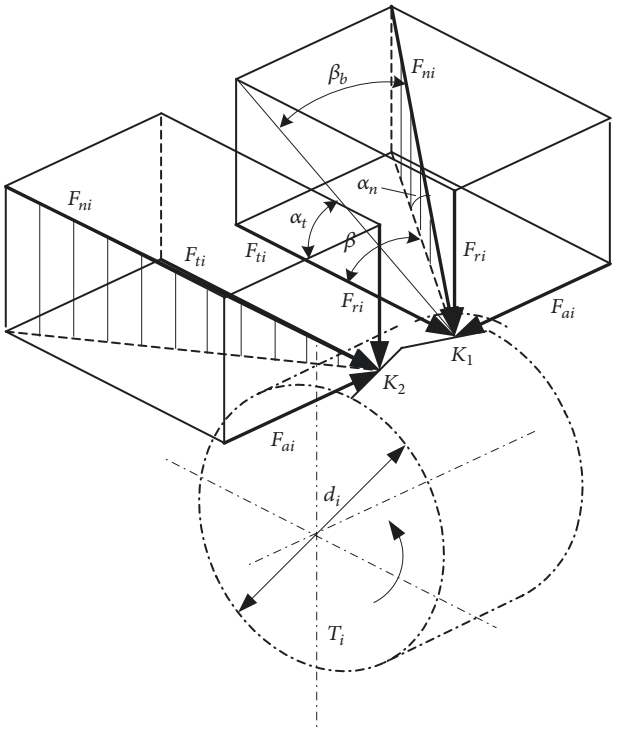

Figure 11: Force analysis of tooth profiles.

Figure 12: Finite element model of single gear teeth.

unit. Because the applied torque is bigger, it will produce approximate two-point contact condition, which conforms to the characteristic of the parabola. Figure 13(a) shows the contact stress result. The contact deformation of tooth profiles is obtained in Figure 13(b). The equivalent stress condition is shown in Figure 13(c) and the equivalent stress will not change suddenly when the gear pair meshes in normal.

Figure 14 shows the maximum contact stress of tooth profiles during meshing process. The maximum contact stress is 763.406MPa, and the minimum contact stress is 476.689MPa. According to the presented results, the teeth mesh at the time of 0.1s and contact position locates on the edge. In the process of 0.2s~0.4s time, gear pair meshes with double teeth. And the single tooth is in mesh after the time 0.5s, while at the time 1.2s the other teeth are in the state of edge contact. When the time is 1.4s, the teeth begin to engage out.

Figure 15 shows the maximum contact deformation of tooth profiles during meshing process. The maximum value is 0.0353mm and the minimum value is 0.0064mm. The maximum and minimum deformation positions locate at the engagement in and out of gear pair.

4. Gear Prototype

Milling method is used to achieve the tooth profiles of gear pair. Utilizing the CNC (Computer Numerical Control) machining center DMU60 (manufactured by Germany DMG), the program of machining codes is developed with

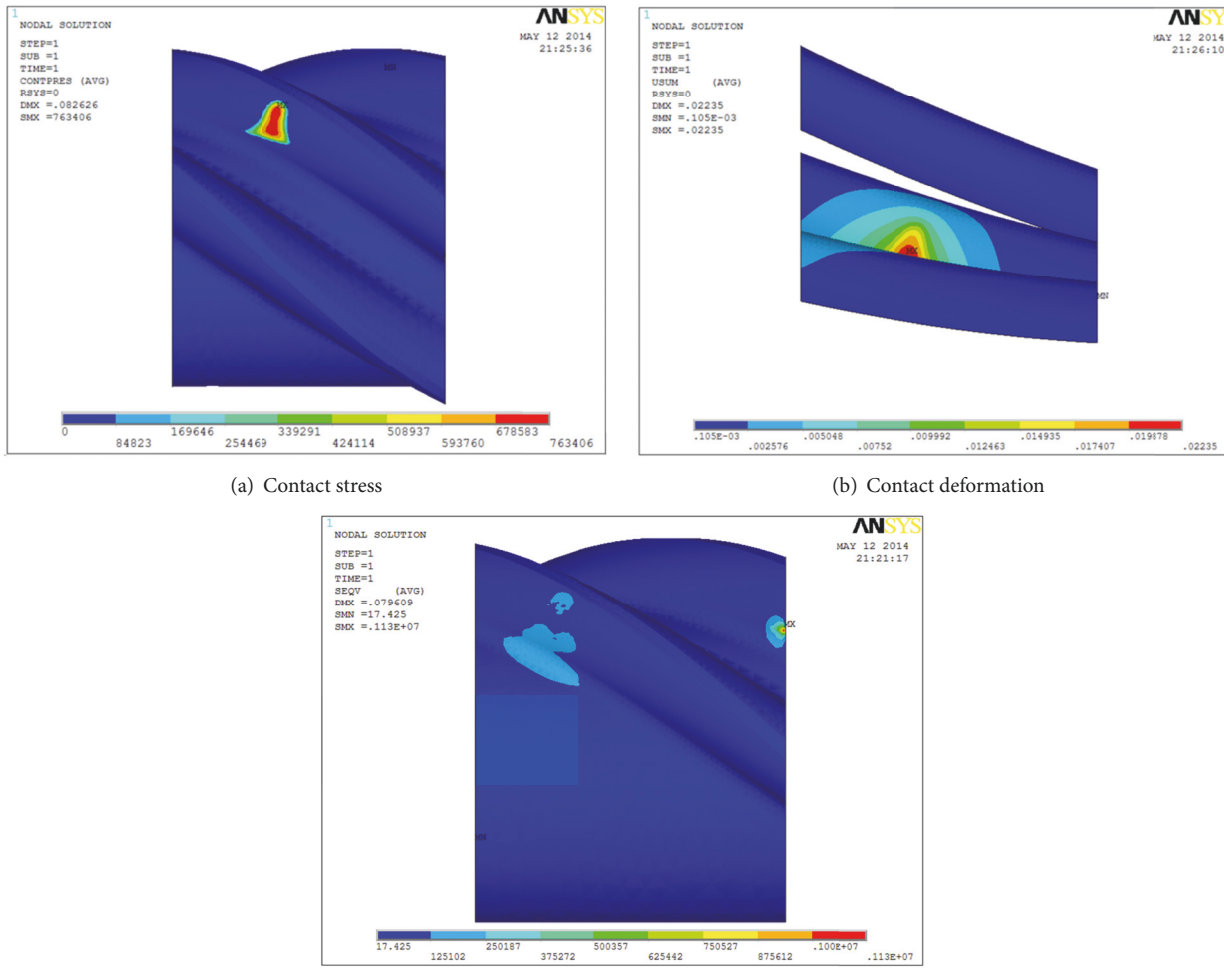

(a) Contact stress

(b) Contact deformation

(c) Equivalent stress

Figure 13: FEA results of tooth profiles.

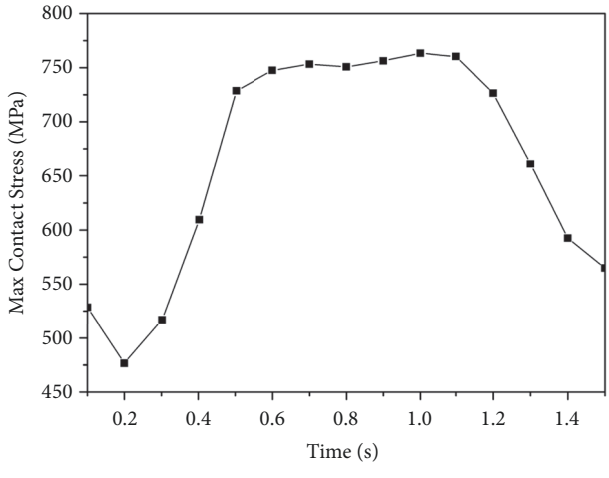

Figure 14: Maximum contact stress during meshing process.

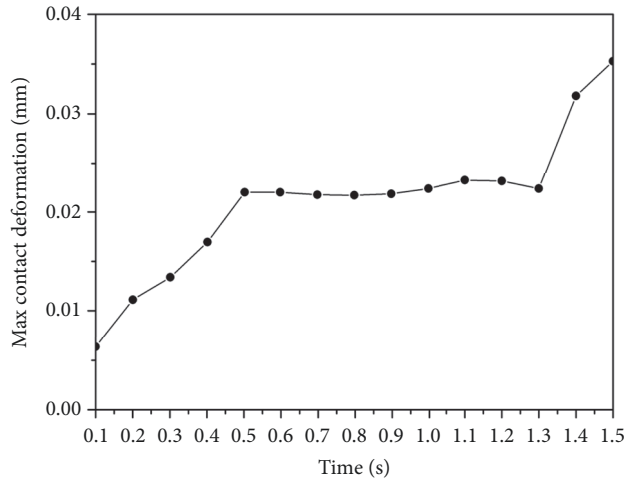

Figure 15: Maximum contact deformation during meshing process.

the ball milling cutter for generating the complex tooth surfaces. The processing of the gear pair is conducted and the generated gear pair is depicted in Figure 16. Further experiments on transmission properties of gear prototypes will be carried out.

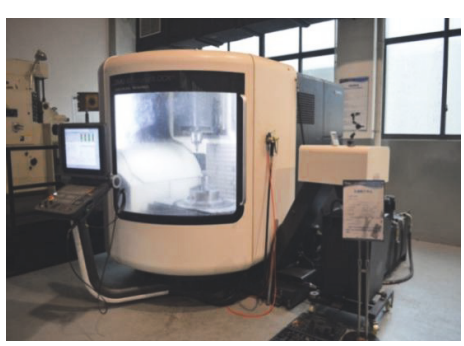

(a) DMU60 machining center

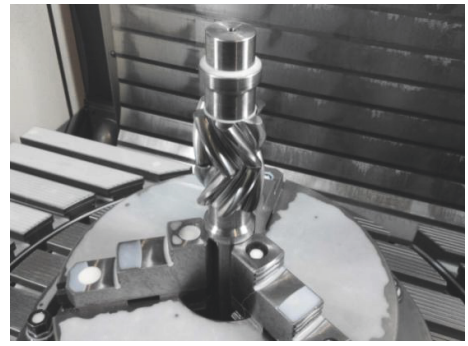

(b) The pinion

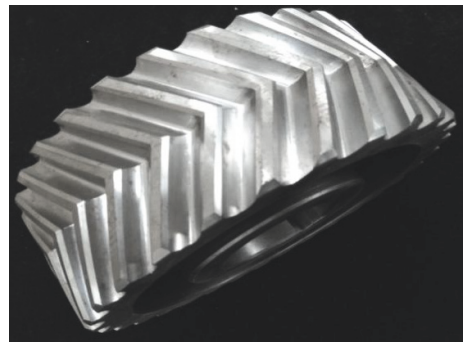

(c) The gear

Figure 16: Gear prototype.

5. Conclusions

(1) Research on the double helical gear transmission with curve element constructed tooth pairs is carried out. The contact curves of tooth profiles include three parts: spatial helix curve Γ_1, spatial helix curve Γ_2, and circular arc curve Γ_3. Generation principle and theoretical mathematical model of tooth profiles are presented based on the geometric relationship. General tooth profiles equations are also derived in terms of equidistance-enveloping approach.

(2) Parametric design of tooth profiles is conducted and numerical example is illustrated according to the developed tooth profiles equations. Solid models of double helical gear pair in terms of given parameters are established. Computerized engagement of tooth profiles is also simulated. The results show that gear pair rotates with a fixed transmission ratio and continuous motion. For the axial direction, tooth profiles mesh in point contact and there is no engagement interference during the mated gear pair.

(3) Force conditions of tooth profiles in the normal direction are analyzed and the normal force in name is expressed using circumferential force, axial force, and radial force. Stress analysis of tooth profiles of gear pair is carried out based on ANSYS software. During the meshing process, the maximum contact stress value is 763.4MPa. The maximum contact deformation value of contact surface is 0.0352mm.

(4) Gear prototypes are manufactured using CNC machining technology. The further tooth contact analysis and dynamic and experimental studies on transmission properties of gear prototypes will be carried out.

Data Availability

The data generated or analyzed during this study are included in this submitted article and the current study data are also available from the corresponding author Dong Liang upon reasonable request.

Conflicts of Interest

The authors declare that they have no conflicts of interest.

Acknowledgments

The research is supported by the National Natural Science Foundation of China (Grant No. 51605049) and Fundamental Research and Frontier Exploration Program of Chongqing City (Grant No. cstc2018jcyjAX0029). Their financial support is grateful acknowledged.

References

[1] A. Fuentes, R. Ruiz-Orzaez, and I. Gonzalez-Perez, "Computerized design, simulation of meshing, and finite element analysis of two types of geometry of curvilinear cylindrical gears," *Computer Methods Applied Mechanics and Engineering*, vol. 272, pp. 321–339, 2014.

[2] L. Dudás, "Modelling and simulation of a new worm gear drive having point-like contact," *Engineering with Computers*, vol. 29, no. 3, pp. 251–272, 2013.

[3] M. Zimmer, M. Otto, and K. Stahl, "Calculation of arbitrary tooth shapes to support gear design," *Proceedings of the Institution of Mechanical Engineers, Part C: Journal of Mechanical Engineering Science*, vol. 231, no. 11, pp. 2075–2079, 2017.

[4] A. Kahraman, "Free torsional vibration characteristics of compound planetary gear sets," *Mechanism and Machine Theory*, vol. 36, no. 8, pp. 953–971, 2001.

[5] S. Li and A. Kahraman, "Prediction of spur gear mechanical power losses using a transient elastohydrodynamic lubrication model," *Tribology Transactions*, vol. 53, no. 4, pp. 554–563, 2010.

[6] V. Simon, "A new worm gear drive with ground double arc profile," *Mechanism and Machine Theory*, vol. 29, no. 3, pp. 407–414, 1994.

[7] V. Simon, "Hob for worm gear manufacturing with circular profile," *The International Journal of Machine Tools and Manufacture*, vol. 33, no. 4, pp. 615–625, 1993.

[8] C.-J. Bahk and R. G. Parker, "Analytical investigation of tooth profile modification effects on planetary gear dynamics," *Mechanism and Machine Theory*, vol. 70, pp. 298–319, 2013.

[9] W. Song, H. Zhou, and Y. Zhao, "Design of the conjugated straight-line internal gear pairs for fluid power gear machines," *Proceedings of the Institution of Mechanical Engineers, Part C: Journal of Mechanical Engineering Science*, vol. 227, no. 8, pp. 1776–1790, 2013.

[10] C. Huang, J.-X. Wang, K. Xiao, M. Li, and J.-Y. Li, "Dynamic characteristics analysis and experimental research on a new type planetary gear apparatus with small tooth number difference," *Journal of Mechanical Science and Technology*, vol. 27, no. 5, pp. 1233–1244, 2013.

[11] C. Lin, L. Zhang, and Z. Zhang, "Transmission theory and tooth surface solution of a new type of non-circular bevel gears," *Journal of Mechanical Engineering*, vol. 50, no. 13, pp. 66–72, 2014 (Chinese).

[12] P. Sondkar and A. Kahraman, "A dynamic model of a double-helical planetary gear set," *Mechanism and Machine Theory*, vol. 70, pp. 157–174, 2013.

[13] H. Zhang, L. Hua, and X. H. Han, "Computerized design and simulation of meshing of modified double circular-arc helical gears by tooth end relief with helix," *Mechanism and Machine Theory*, vol. 45, no. 1, pp. 46–64, 2010.

[14] C. Wang, Z.-D. Fang, H.-T. Jia, and J.-H. Zhang, "Modification optimization of double helical gears," *Journal of Aerospace Power*, vol. 24, no. 6, pp. 1432–1436, 2009.

[15] K. Kawasaki, I. Tsuji, and H. Gunbara, "Manufacturing method of double helical gears using multi-axis control and multi-tasking machine tool," in *International Gear Conference*, pp. 86–95, 2014.

[16] K. Kawasaki, I. Tsuji, and H. Gunbara, "Manufacturing method of double-helical gears using CNC machining center," *Proceedings of the Institution of Mechanical Engineers, Part C: Journal of Mechanical Engineering Science*, vol. 230, no. 7-8, pp. 1149–1156, 2015.

[17] B. Chen, D. Liang, and Y. Gao, "The principle of conjugate curves for gear transmission," *Journal of Mechanical Engineering*, vol. 50, no. 1, pp. 130–136, 2014 (Chinese).

[18] B. Chen, Y. Gao, and D. Liang, "Tooth profile generation of conjugate-curve gears," *Journal of Mechanical Engineering*, vol. 50, no. 3, pp. 18–24, 2014 (Chinese).